

Microvascular blood-brain barrier alterations in isolated brain capillaries of mice over-expressing alpha-synuclein (Thy1-aSyn line 61)

Kristina Lau^{a,b,1}, Lisa T. Porschen^{a,1}, Franziska Richter^{a,b,*}, Birthe Gericke^{a,b,*}

^a Department of Pharmacology, Toxicology and Pharmacy, University of Veterinary Medicine Hannover, Bünteweg 17, 30559 Hannover, Germany

^b Center for Systems Neuroscience, Hannover, Germany

ARTICLE INFO

Keywords:

Synucleinopathies
Parkinson's disease
Brain capillaries
Aquaporin
Tight junctions
Endothelial activation

ABSTRACT

Dysfunction of the blood-brain barrier (BBB) is suggested to play a critical role in the pathological mechanisms of Parkinson's disease (PD). PD-related pathology such as alpha-synuclein accumulation and inflammatory processes potentially affect the integrity of the BBB early in disease progression, which in turn may alter the crosstalk of the central and peripheral immune response. Importantly, BBB dysfunction could also affect drug response in PD. Here we analyzed microvascular changes in isolated brain capillaries and brain sections on a cellular and molecular level during disease progression in an established PD mouse model that overexpresses human wild-type alpha-synuclein (Thy1-aSyn, line 61). BBB alterations observed in Thy1-aSyn mice included reduced vessel density, reduced aquaporin-4 coverage, reduced P-glycoprotein expression, increased low-density lipoprotein receptor-related protein 1 expression, increased pS129-alpha-synuclein deposition, and increased adhesion protein and matrix metalloprotease expression together with alterations in tight junction proteins. Striatal capillaries presented with more dysregulated BBB integrity markers compared to cortical capillaries. These alterations of BBB integrity lead, however, not to an overt IgG leakage in brain parenchyma. Our data reveals intricate alterations in key proteins of BBB function together with histological evidence for altered structure of the brain vasculature. Thy1-aSyn mice represent a useful model to investigate therapeutic targeting of BBB alterations in synucleinopathies.

1. Introduction

Alpha-synuclein accumulation and aggregation in brain cells is the common denominator of synucleinopathies, such as Parkinson's disease (PD), Dementia with Lewy bodies (DLB) and Multiple system atrophy (MSA) (McCann et al., 2014; Spillantini et al., 1998). PD is the second most common neurodegenerative disorder with exponentially increasing incidence in the aging population (Dorsey and Bloem, 2018). While current therapy effectively alleviates many symptoms caused by dopamine loss due to degeneration of dopaminergic neurons in the substantia nigra pars compacta, there is still no treatment to halt or modify the progression of underlying disease mechanisms (Chiu et al., 2022; Devos et al., 2021; Zeuner et al., 2019). Alpha-synuclein related pathology is a rational target for therapy development based on (i) the presence of alpha-synuclein accumulation in Lewy bodies, a pathological hallmark of synucleinopathies (Spillantini et al., 1997), (ii) the fact

that multiplication of SNCA causes familial forms of PD, and (iii) the observation that polymorphisms in non-coding regions of SNCA increase PD risk or progression (Edwards et al., 2010; Gatto et al., 2010; Huang et al., 2011).

Compounds currently in pre-clinical and clinical trials such as small molecules, antibodies or enzymes are required to cross the blood-brain barrier (BBB). However, the BBB is altered substantially with aging and thus expected to be compromised in age-related neurodegenerative diseases (Hou et al., 2019; Zhao et al., 2015). In fact, BBB alteration may contribute to disease pathogenesis. The neurovascular unit is formed by endothelial cells linked by tight junctions, enclosed by a basal lamina and encircled by pericytes, astrocytic endfeet and the immediate surrounding brain parenchyma with microglia and neurons (Abbott, 2013; Daneman et al., 2010). By integration of highly specific transporter systems, the BBB represents a selectively permeable membranous barrier imperative to healthy brain function. With aging, the BBB integrity

* Corresponding authors at: Department of Pharmacology, Toxicology and Pharmacy, University of Veterinary Medicine Hannover, Foundation, Bünteweg 17, 30559 Hannover, Germany.

E-mail addresses: kristina.lau@tiho-hannover.de (K. Lau), franziska.richter@tiho-hannover.de (F. Richter), birthe.gericke@tiho-hannover.de (B. Gericke).

¹ Equal contribution.

<https://doi.org/10.1016/j.nbd.2023.106298>

Received 8 May 2023; Received in revised form 22 August 2023; Accepted 13 September 2023

Available online 15 September 2023

0969-9961/© 2023 The Author(s). Published by Elsevier Inc. This is an open access article under the CC BY license (<http://creativecommons.org/licenses/by/4.0/>).

decreases, e.g. via loss of function of P-glycoprotein (P-gp), an important efflux transporter (van Assema et al., 2012). Imaging studies suggested that P-gp function is decreased in advanced PD compared to age-matched controls in brainstem, cerebellar tonsils, frontal regions, substantia nigra and midbrain (Bartels et al., 2008; Kortekaas et al., 2005), but was also found to be upregulated in de novo PD in midbrain and substantia nigra (Bartels et al., 2008). Post-mortem pathology reports alterations of the microstructure of capillaries (Farkas et al., 2000) and BBB leakiness (Gray and Woulfe, 2015). It is unclear whether this compromised function of the barrier contributes to progression of neurodegeneration, e.g. by increased transition of peripheral toxins, cytokines or immune cells. Of note, if alpha-synuclein accumulates and aggregates at the BBB, then this may interfere with penetration of alpha-synuclein targeted therapeutic compounds. Therefore, it is imperative to investigate whether alpha-synuclein pathology at the neurovascular unit coincides with impairment of the BBB early in PD progression.

In brain sections of mice over-expressing A53T mutated (under the prion promoter) or wild-type alpha-synuclein (under the bacterial artificial chromosome (BAC)-alpha-synuclein-green fluorescent protein (GFP) construct), a decreased expression of tight junction proteins and a leakage of the BBB were observed among other alterations (Elabi et al., 2021; Lan et al., 2022). Characterization of BBB integrity requires molecular analysis specifically in brain capillaries as opposed to whole brain tissue extracts or sections. Here we provide an in depth quantification of the expression of cell adhesion, tight junction and transporter proteins in isolated brain capillaries derived from an established model of synucleinopathies with over-expression of wild-type alpha-synuclein (Thy1-aSyn line 61 mice) at two prodromal progression stages (Hartlage-Rubsamen et al., 2021; Richter et al., 2023; Schidlitzki et al., 2023).

2. Materials and methods

2.1. Animals

Thy1-aSyn (line 61) transgenic mice over-expressing human wild-type alpha-synuclein under the Thy-1 promoter were maintained on a mixed C57BL/6-DBA/2 background as described previously (Richter et al., 2023). Polymerase chain reaction (PCR) amplification analysis was performed on ear tissue samples collected both at birth and at the completion of the experiment. Only mice with confirmed genotypes were included in the analyses. Animals were treated according to the EU council directive 2010/63/EU and the German Law on Animal Protection with approvals for breeding and the procedures by the respective government agency (Lower Saxony State Office for Consumer Protection and Food Safety). All efforts were made to minimize both the suffering and the number of animals. All animal experiments of this study were conducted and are reported in accordance with ARRIVE guidelines.

Only male transgenic mice and age-matched wild-type animals were used. Due to the location of the transgene on the X-chromosome and random inactivation, female Thy1-aSyn mice express less transgene and show no or subtle phenotypes (Gerstenberger et al., 2016). Littermates of the same sex were housed together at a maximum occupancy of four mice per cage under specific pathogen free conditions in open lid cages. Animals were maintained on a reverse 12 h dark/light cycle, and food (standard rodent chow or medicated food admix) and water ad libitum. Sample sizes were determined based on a priori power analysis (Cheslelet et al., 2012). Per group 5 animals were used for experiments requiring capillary isolation and 8 animals per group for immunohistochemistry ($n = 5$ /group capillary isolation, $n = 8$ /group immunohistochemistry). Two different time points of progression were compared, 2 and 6 months of age. At 2 months of age, Thy1-aSyn mice develop alpha-synuclein pathology especially in the striatum and substantia nigra, and show early sensorimotor deficits. At 6 months of age Thy1-aSyn mice represent a model of prodromal PD with motor and non-motor dysfunction, alpha-synuclein pathology, nigrostriatal microgliosis and increased extracellular dopamine and dopamine metabolism. Dopamine

loss and symptoms of Parkinsonism become significant at 14–16 months of age. As a positive control for immunoglobulin G (IgG) leakage into brain parenchyma the cortices of wild-type and Thy1-aSyn mice ($n = 1$) injected with a single dose of 0.8 mg/kg i.p. lipolysaccharide (LPS) were used. 3 days post-injection the animals were euthanized by an overdose of pentobarbital followed by transcardiac perfusion and brain removal as described in immunohistochemistry section.

2.2. Brain capillary isolation

Brain microvessels were isolated from striata and cortices of mice from different genotypes (Thy1-aSyn and wild-type, WT) and age groups (2 and 6 months) as described previously (Puris et al., 2022). Therefore, brains were removed immediately after carbon dioxide exposure and decapitation. Brains were cleaned from meninges and large superficial blood vessels by rolling on sterile tissue sheets (Whatman, VWR). Striata and cortices were dissected and homogenized separately with a Dounce homogenizer and 20 up and down strokes in 5 volumes of buffer A (101 mM NaCl, 4.6 mM KCl, 5 mM CaCl₂, 1.2 mM KH₂PO₄, 1.2 mM MgSO₄, 15 mM HEPES, 5 mM D-glucose, 1 mM sodium pyruvate, pH 7.4) per gram of tissue. All isolation steps were carried out on ice. The homogenate was centrifuged at 2000 xg, 10 min, 4 °C and the resulting pellet was suspended in buffer B (buffer A containing 16% dextran, Sigma-Aldrich). First the suspension and then the resulting supernatant were centrifuged at 2000 xg, 10 min, 4 °C in a swinging bucket rotor without break. The pellets from both centrifugation steps were pooled in 10 mL buffer C (buffer A supplemented with 0.5% bovine serum albumin) and sequentially passed through cell strainers with mesh sizes of 200 μm, 100 μm and 30 μm. Brain capillaries trapped on the 30 μm mesh were collected by washing with 40 mL buffer C followed by centrifugation at 1000 xg, 10 min, 4 °C. The microvessel pellet was suspended in 1 mL of buffer A and 5–10 μL of the isolated brain capillary fraction was observed under a light microscope to ensure purity, and processed for immunohistochemistry. Isolated microvessels appeared in morphology and size as capillaries as expected, and are therefore referred to as such in the following chapters. The remaining suspension was centrifuged again at 1000 xg, 10 min, 4 °C and supernatant was completely removed. Pellets were snap frozen at –80 °C or directly used for downstream western blot analysis.

2.3. Phase-contrast microscopy and immunofluorescent staining of isolated brain capillaries

Enrichment and purity of the isolated brain capillary suspension were evaluated using a Zeiss microscope (Inverted ZEISS Axio Vert.A1 microscope, Carl Zeiss Microscopy GmbH, Germany). Therefore, 5 μL from suspension of freshly isolated brain capillaries were transferred onto an object slide and analyzed using a 20× magnification objective and phase-contrast. Images were processed using ZEISS 3.0 blue edition (ZEN lite, Version 10.0.19044, Carl Zeiss Microscopy GmbH, Germany).

For immunofluorescent staining isolated brain capillaries were mounted on poly-D-lysine (50 μg/mL in PBS) coated microscope slides and fixed with 4% paraformaldehyde (PFA) for 15 min. After permeabilization with 1% Triton X-100 in PBS for 15 min and blocking in 2% BSA in PBS for 30 min samples were incubated with primary antibodies at room temperature (RT) for 1 h in PBS containing 2% BSA, 0.5% saponin and 0.1% Triton X-100, followed by incubation with secondary Alexa Fluor coupled antibodies for 1 h at RT. For antibodies and dilutions, see table S1. After washing, coverslips were finally mounted in Prolong Gold antifade (Carl Roth, Karlsruhe, Germany) including 4',6-diamidino-2-phenylindol (Dapi) as a nuclear counterstain. Samples were examined by a Leica TCS SP5 II confocal microscope (Leica Microsystems, Bensheim, Germany) with a HCXPL APO 63× lambda blue 1.4 oil immersion objective. Excitation wavelengths of 405 nm (Dapi), 530 nm (alpha-synuclein) and 633 nm (collagen IV) were used.

2.4. Analysis of pericyte number on isolated brain capillaries

Brain capillaries isolated from striatum or cortex of Thy1-aSyn and WT mice aged 2 or 6 months ($n = 3$ per group) were visualized by immunofluorescent staining for collagen IV (basement membrane) and nuclear counterstain with Dapi, followed by confocal laser scanning microscopy as described in the previous section. Cell numbers were determined independently by two investigators in a blinded fashion by counting pericytes in relation to endothelial cells on 14–42 images per mouse and brain region. Pericytes were differentiated from microvascular endothelial cells according to following criteria: abluminal localization of pericytes, pericyte cell body delineated by collagen IV staining and nuclear staining with Dapi. Endothelial cells can be identified by elongated cell nuclei in the capillary lumen. Finally, the ratio of pericytes to endothelial cells was calculated.

2.5. Western blot analysis of brain capillaries

Freshly isolated brain capillaries were lysed in 30 μ L radioimmunoprecipitation assay (RIPA) buffer (20 mM Tris, 50 mM NaCl, 0.5% (w/v) sodium deoxycholate, 0.5% (v/v) Triton X-100, pH 8.0) supplemented with complete protease inhibitor and phosSTOP (Roche, Mannheim, Germany) on ice by passage through a 23 G syringe needle. For zonula occludens-1 (ZO-1) protein expression measurement cortical and striatal brain homogenate was used. Lysates were cleared by centrifugation and protein concentration of the samples was determined using Pierce BCA Protein Assay kit (Thermo Fisher Scientific, Darmstadt, Germany). Equal amounts of protein (2.5 μ g) were separated by sodium dodecyl sulfate-polyacrylamide gel electrophoresis using 4–20% Mini Protean gels (Bio-Rad), transferred to a polyvinylidene difluoride membrane and incubated in 5% non-fat milk (w/v) in PBS-T (PBS +0.05% Tween 20) for 1 h at RT for blocking. Prior to blocking, membranes for alpha-synuclein and alpha-synuclein phosphorylated at serine129 (pS129) detection were additionally incubated in PBS with 0.4% PFA for 30 min at RT followed by washing with PBS-T. After blocking, membranes were incubated with primary antibodies for 1 h at RT. Primary antibodies and dilutions used are listed in table S1. For ZO-1, the $\alpha +$ and $\alpha -$ isoforms were detected (Willott et al., 1992). After washing, secondary antibody incubation was performed with either polyclonal goat anti-rabbit (1:1000; Dako, Hamburg, Germany, cat. #P0448) or polyclonal goat anti-mouse (1:1000; Dako, cat. #P0260) for 1 h at RT. Protein bands were visualized using SuperSignal West Femto Chemiluminescent Substrate (Thermo Fisher Scientific) and the Chemidoc™ XRS Imager (Bio-Rad Laboratories, Munich, Germany). Protein bands were quantified using ImageLab version 6.0.1 (Bio-Rad, Hercules, CA, USA). Protein expression is presented as intensity of target protein bands normalized to total protein visualized by stain-free technology (Bio-Rad).

2.6. Immunohistochemistry of brain tissue sections

For immunohistochemical analysis of brain slices, mice ($n = 8$ each wild-type and Thy1-aSyn mice) were euthanized by an overdose of pentobarbital followed by sequential transcardiac perfusion with PBS followed by 4% PFA. Brains were quickly removed from the skull, post-fixed in 4% PFA for 24 h, cryoprotected in 10–30% gradient of sucrose in 0.1 M PBS and stored at 4 °C until cutting. Frozen brains were cut into 40 μ m thick coronal sections on a cryostat. Fluorescent staining was performed in two brain sections per mouse of striatum, substantia nigra and hippocampus, cortex was analyzed in the same brain sections. For aquaporin-4 (AQP4) immunostaining, sections were blocked with goat serum and incubated with primary antibody overnight at 4 °C. After incubation with secondary antibody for 1 h, DyLight649-conjugated *Lycopersicon esculentum* (tomato) lectin (LEL, TL) was added overnight at 4 °C. For lectin and IgG immunostaining, brain sections were blocked with donkey serum followed by incubation with primary fluorescent-

labeled antibodies overnight at 4 °C. After immunostaining sections were mounted on glass slides using ProLong™ Gold Antifade Mountant with Dapi (Thermo Fischer). Primary and secondary antibodies used are listed in table S1. Image acquisition was performed using Zeiss Axio Observer 7 microscope equipped with an Axiocam 506, a Zeiss Colibri 7 LED light source and either 20 \times or 40 \times magnification lenses. The Apotome Cam function was additionally used for IgG stained sections. Images were taken as Z-stacks with an interval of 1.0 μ m.

2.7. Image analysis for aquaporin-4, lectin and IgG leakage

For brain vessel or AQP4 density analysis the respective fluorescent channel was chosen and six z-stack images from each brain region ($n = 8$, striatum, substantia nigra, hippocampus, cortex) were transferred to a maximum projection. After thresholding percentage of AQP4⁺ or lectin⁺ pixels on the images were measured using the area fraction measurement tool from Fiji package of ImageJ (Schindelin et al., 2012).

BBB integrity was analyzed by double fluorescence labeling using DyLight649-conjugated *L. esculentum* lectin to label vascular endothelium and a specific mouse IgG antibody to detect serum leakage by perivascular IgG signal. IgG serum leakage was examined in two sections of each brain region (striatum, substantia nigra, hippocampus, cortex) under the Zeiss Axio Observer 7 microscope and frequency of areas with IgG positive serum leakage was counted per group (WT vs. Thy1-aSyn).

2.8. Statistics

Data is presented as mean \pm standard error of the mean (SEM). Statistical significance was calculated using GraphPad Prism 9.01 software (GraphPad Software, United States). To assess statistical significance for non-parametric data, we used the Mann-Whitney test comparing between genotypes (WT, Thy1-aSyn) and age (2-, 6-month-old). Brain regions were processed separately and are therefore not compared statistically. Statistical significance was indicated by * $p < 0.05$ and ** $p < 0.01$ as determined by statistical tests.

3. Results

3.1. Lower brain capillary density and AQP4⁺ astrocytic endfeet coverage in Thy1-aSyn mice

Prior to analyzing isolated capillaries, we determined their density in brain sections of different brain regions from 6 months old Thy1-aSyn mice (prodromal phase with alpha-synuclein pathology most pronounced in nigrostriatal system) compared to wild-type animals (Fig. 1A, B). Density of lectin-positive capillaries (Fig. 1A) was significantly decreased in dorsal striatum of transgenic mice but not in cortex, substantia nigra or hippocampus (Fig. 1B). To further describe this potential BBB alteration, astrocyte endfeet surrounding brain capillaries were visualized by the water channel AQP4 as an index for astrocyte-vascular coupling (Fig. 1A) (Halder and Milner, 2020). As expected, AQP4 showed exclusive localization to lectin stained brain vessels (overlay Fig. 1A). Quantification revealed decreased AQP4 coverage of brain capillaries in striatum and cortex of Thy1-aSyn mice compared to wild-type (Fig. 1C).

3.2. No change in brain capillary pericyte to endothelial cell ratio in Thy1-aSyn mice

Pericytes are vascular mural cells that cover the abluminal surface of capillaries and support BBB integrity (Fig. 1D and E). To assess pericyte coverage in Thy1-aSyn mice, pericyte to endothelial cell ratio was determined. As described previously for brain capillaries (Pardridge, 1999), the ratio was confirmed to be $\sim 1:3$ in both genotypes and age groups indicating no changes in capillary associated pericyte number in 2 and 6 months old Thy1-aSyn mice (ratios: WT, 2 months cortex: 1:3;

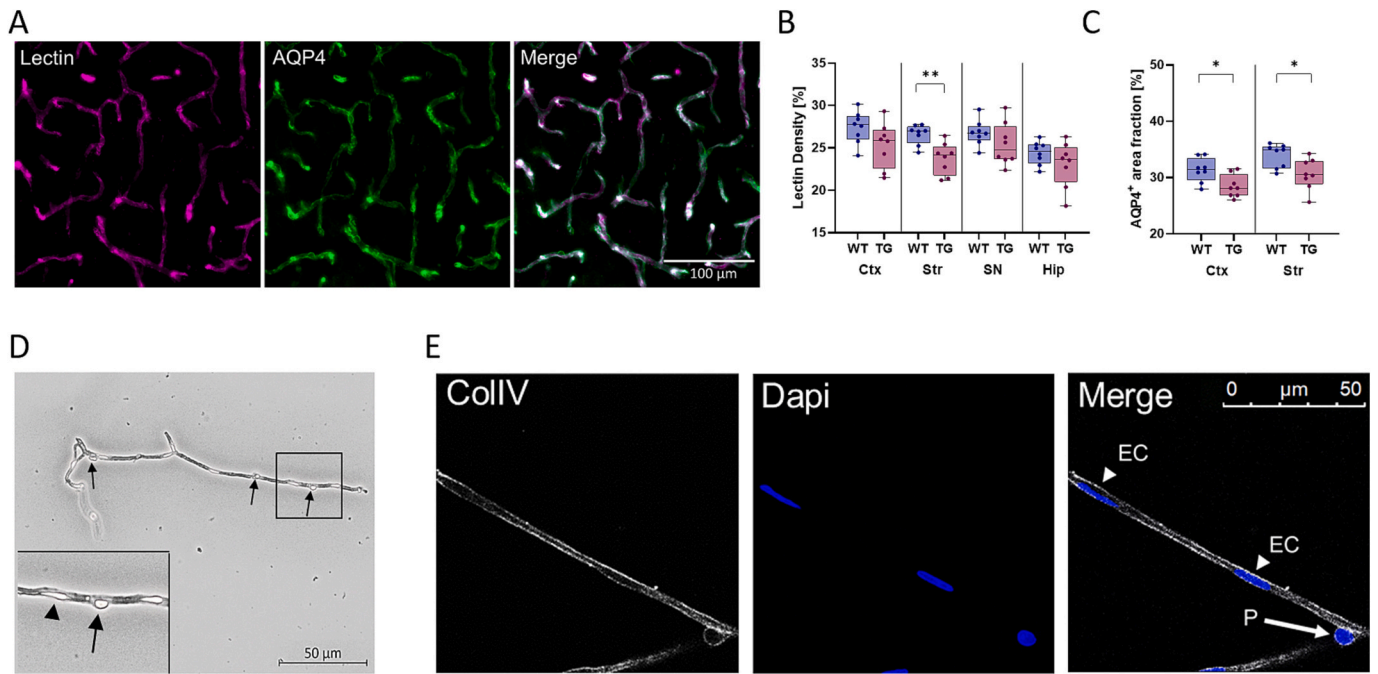


Fig. 1. Capillary density, aquaporin-positive astrocytic endfeet coverage and capillary associated pericyte number in different brain regions of Thy1-aSyn mice. (A) Representative fluorescent images of brain capillaries stained by lectin (magenta) and aquaporin-4 (AQP4) in astrocytic endfeet (green) in the striatum of a 6 months old Thy1-aSyn mouse. (B) Measurement of capillary density in 4 different brain regions (Ctx: cortex, Str: striatum, SN: substantia nigra, Hip: hippocampus) of Thy1-aSyn transgenic mice (TG) compared to wild-type (WT) animals ($n = 8$ animals/group) at the age of 6 months. (A,B) All values are presented as mean \pm SEM ($n = 8$ /group), individual data points are shown. $*p < 0.05$, $**p < 0.01$, Mann-Whitney test. (C) Coverage of brain capillaries by AQP4-positive astrocytic endfeet by analysis of AQP4 area fraction in Ctx and Str of 6 months old WT and Thy1-aSyn mice. (D, E) Isolated cortical brain capillaries from Thy1-aSyn mouse brain and differentiation of endothelial cells and pericytes by localization and morphology. (D) Phase-contrast micrograph of freshly isolated cortical brain capillaries from a Thy1-aSyn mouse brain. The framed region is magnified in the lower left corner. Pericytes attached to the outer capillary surface are highlighted by arrows and can be differentiated from luminal endothelial cells lining the luminal side of the capillaries and visible by elongated cell nuclei (arrowheads, magnification). (E) Immunofluorescent staining of paraformaldehyde fixed brain capillaries for cell nuclei (blue) and capillary basement membrane by collagen IV staining (ColIV, white). EC: endothelial cell, P: pericyte. (For interpretation of the references to colour in this figure legend, the reader is referred to the web version of this article.)

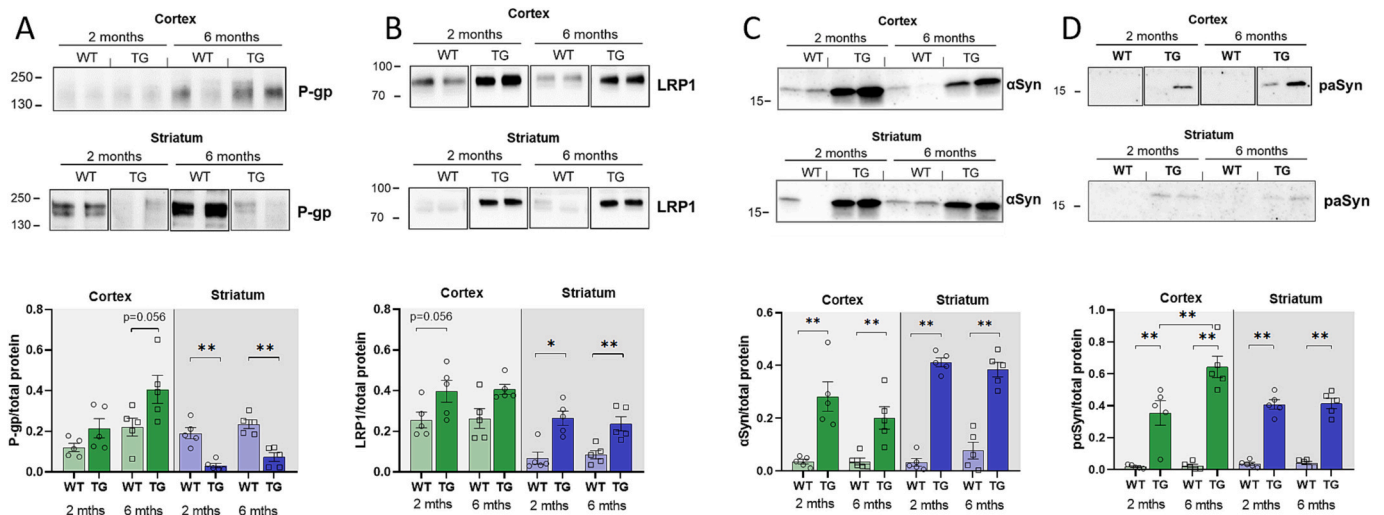


Fig. 2. Differential protein expression of toxin transporter P-glycoprotein (P-gp) and potential alpha-synuclein receptor low-density lipoprotein receptor-related protein 1 (LRP1) and alpha-synuclein (aSyn) and phosphorylated alpha-synuclein (paSyn) deposition in brain capillaries of Thy1-aSyn mice vs wild-type. Representative western blot showing P-gp (A), LRP1 (B), aSyn (C) and pS129-alpha-synuclein (D) protein levels in brain capillaries isolated from cortex or striatum of single Thy1-aSyn (TG) or wild-type (WT) animals at 2 and 6 months (mths) of age and quantification analysis of protein band intensity normalized to total protein. (A,B,C,D) Protein size is expressed in kDa. Borders indicate different blots, lines indicate sliced blots as 2 out of 3 samples are shown. Images of the full unprocessed gels and blots are provided in the supplemental data. All values are represented as mean \pm SEM ($n = 5$ /group), individual data points are shown. $*p < 0.05$, $**p < 0.01$, Mann-Whitney test.

WT, 2 months, striatum: 1:4; Thy1-aSyn, 2 months, cortex: 1:3; Thy1-aSyn, 2 months, striatum: 1:3; WT, 6 months, cortex: 1:4; WT, 6 months, striatum: 1:4; Thy1-aSyn, 6 months, cortex: 1:3; Thy1-aSyn, 6 months, striatum: 1:3).

3.3. Downregulation of P-gp, upregulation of LRP1 and pS129-alpha-synuclein deposition in Thy1-aSyn brain capillaries

The active efflux transporter P-glycoprotein (P-gp) and the low-density lipoprotein receptor-related protein 1 (LRP1) contribute critically to a functional BBB (Storck et al., 2021; van Assema et al., 2012). P-gp expression was overtly downregulated in capillaries from striatum of Thy1-aSyn mice at 2 and 6 months of age compared to wild-type, but not in cortical capillaries, which rather tended to upregulate P-gp expression (Fig. 2A). Conversely, LRP1 protein expression was upregulated in brain capillaries from striatum of Thy1-aSyn mice independent of age. Wild-type mice appear to express high levels of LRP1 in cortical compared to striatal capillaries, with a trend to increase in Thy1-aSyn mice (Fig. 2B). P-gp is localized at the luminal side of the endothelium and extrudes xenobiotics from brain to blood whereas LRP1 is described to be involved in alpha-synuclein transport across the BBB (Miller et al., 2000; Sui et al., 2014). To determine if increased LRP1 expression correlates with increased alpha-synuclein deposition and pathology we determined the level of mouse and human alpha-synuclein protein and alpha-synuclein phosphorylated at serine129 (pS129), which associates with potentially toxic aggregates (Fujiwara et al., 2002). As supposed, Thy1-aSyn mice accumulate alpha-synuclein in striatal but also in cortical brain capillaries (Fig. 2C) at 5- to 12-fold increase in protein level. Importantly, brain capillaries of Thy1-aSyn mice also accumulate the pS129-alpha-synuclein post-translational modification, with progression between 2 and 6 months of age in the cortex (Fig. 2D).

3.4. Endothelial activation: brain region specific upregulation of cell adhesion molecules (CAMs)

Reduction in efflux transporter and accumulation of pS129-alpha-synuclein indicate pathological processes in the neurovascular unit, which could co-occur with endothelial cell specific inflammatory processes. Therefore, we quantified cell adhesion molecules involved in immune-mediated inflammatory processes in the endothelium. Western blot analysis of brain capillaries for vascular cell adhesion molecule 1 (VCAM-1) revealed an upregulation in striatal but not in cortical capillaries isolated from Thy1-aSyn mice of both age groups (Fig. 3A). Conversely, the intercellular adhesion molecule 1 (ICAM-1) was upregulated in cortical but not in striatal capillaries from Thy1-aSyn mice (Fig. 3B). The expression of matrix metalloprotease-3 (MMP-3), described to be upregulated under inflammatory/pathological conditions (Buzhdygan et al., 2020; Chung et al., 2013; McClain et al., 2009), is increased in striatal brain capillaries of Thy1-aSyn mice, but not in the cortex, where its expression even decreases with age (Fig. 3C).

3.5. Regionally specific alterations in tight junction and matrix metalloprotease protein expression

Paracellular flux at the BBB is strictly regulated by endothelial cell tight junction proteins including occludin (Ocln), claudin-5 (Cldn5) and zonula occludens-1 (ZO-1) (Gericke et al., 2020; Luissint et al., 2012). MMPs are involved in degradation of tight junction proteins especially under pathological conditions, therefore increase in striatal MMP-3 expression could impact tight junction integrity (Hartz et al., 2012; Rempe et al., 2018). Accordingly, western blot analysis of striatal capillaries showed a reduction in Ocln expression in Thy1-aSyn mice at 2 months of age. The reduction of expression in wild-type with age precluded significance of reduction at 6 months of age (Fig. 4A). Interestingly, cortical capillaries upregulated Ocln expression in Thy1-aSyn mice and with age (Fig. 4A). An increase of expression with age in cortical capillaries was also apparent for Cldn5 in Thy1-aSyn mice,

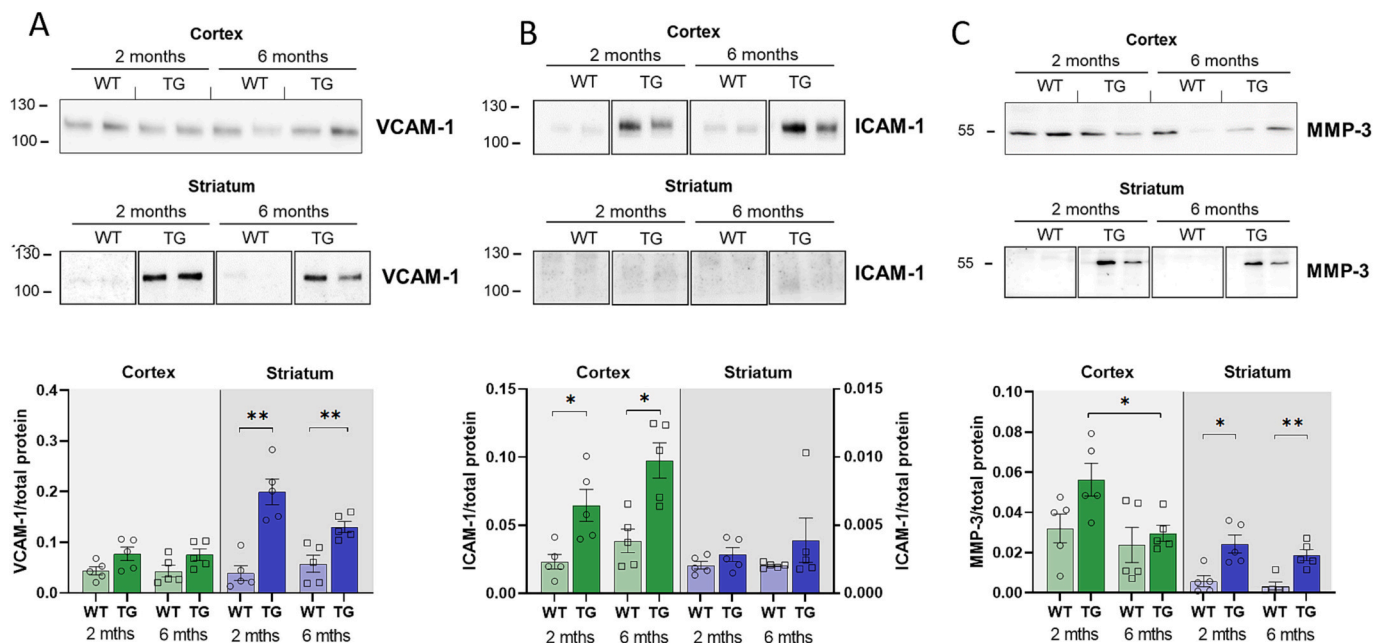


Fig. 3. Brain region specific upregulation of cell adhesion molecules (CAMs) and matrix metalloprotease-3 (MMP-3) in brain capillaries of Thy1-aSyn animals. Representative western blot showing VCAM-1 (A), ICAM-1 (B) and MMP-3 (C) protein levels in brain capillaries isolated from cortex or striatum of single Thy1-aSyn (TG) or wild-type (WT) animals at 2 and 6 months (mths) of age and quantification analysis of protein band intensity normalized to total protein. (A,B,C) Protein size is expressed in kDa. Borders indicate different blots, lines indicate sliced blots as 2 out of 3 samples are shown. Images of the full unprocessed gels and blots are provided in the supplemental data. All values are represented as mean ± SEM (n = 5/group), individual data points are shown. *p < 0.05, **p < 0.01, Mann-Whitney test. VCAM-1: vascular cell adhesion molecule 1, ICAM-1: intercellular adhesion molecule 1.

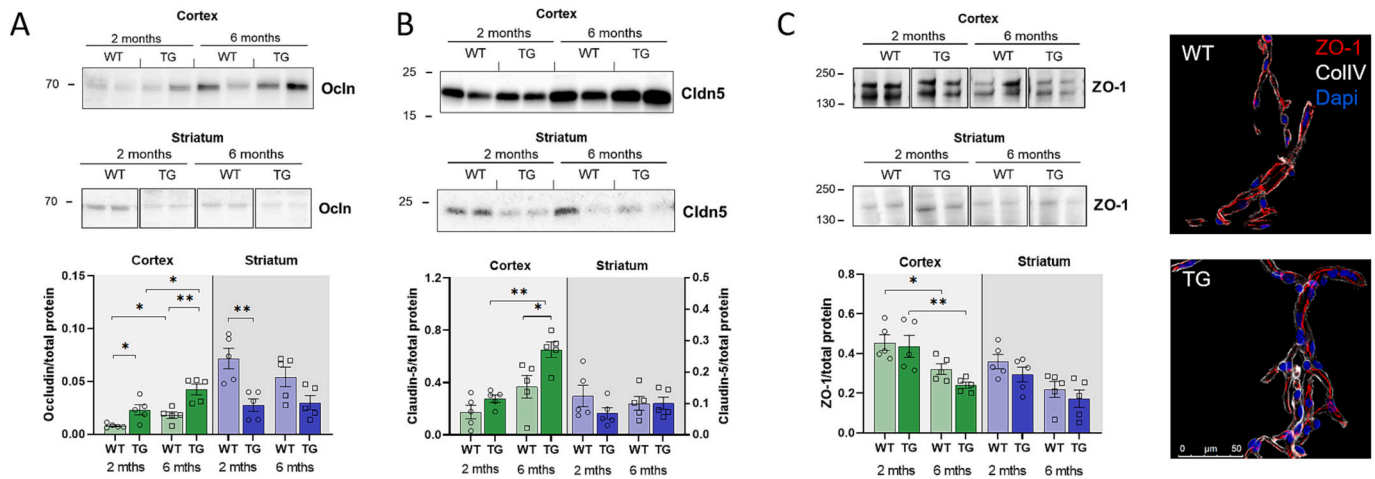


Fig. 4. Tight junction protein expression levels in brain capillaries of Thy1-aSyn mice. Protein lysates of isolated brain capillaries from striatum and cortex of Thy1-aSyn (TG) and wild-type (WT) animals (n = 5) at 2 and 6 months (mths) of age and total brain homogenate of cortex and striatum for zonula occludens-1 (ZO-1) detection were subjected to western blotting to measure protein levels of occludin (Ocn) (A), claudin-5 (Cldn5) (B), and zonula occludens-1 (ZO-1) α + and α -isoforms (C). Representative western blots and quantification of normalized band intensities are depicted. (A,B,C) Protein size is expressed in kDa. Borders indicate different blots, lines indicate sliced blots as 2 out of 3 samples are shown. Images of the full unprocessed gels and blots are provided in the supplemental data. All values are represented as mean \pm SEM (n = 5/group), individual data points are shown. *p < 0.05, **p < 0.01, Mann-Whitney test. (C) Representative fluorescence microscopy image shows isolated brain capillaries from striatum of a 2 months old wild-type (WT) and Thy1-aSyn (TG) mouse stained for ZO-1 (red), the basement membrane by collagen IV (ColIV, white) and nuclei using Dapi (blue). (For interpretation of the references to colour in this figure legend, the reader is referred to the web version of this article.)

leading to higher Cldn5 levels compared to wild-type at 6 months of age (Fig. 4B). Conversely, Cldn5 levels in striatal capillaries were unaffected by age or genotype. Finally, ZO-1 expression decreased with age in

cortical brain homogenate in both genotypes, further confirming an age-related alteration of tight junction proteins in the cortex. There was no difference between Thy1-aSyn and wild-type mice in ZO-1 expression

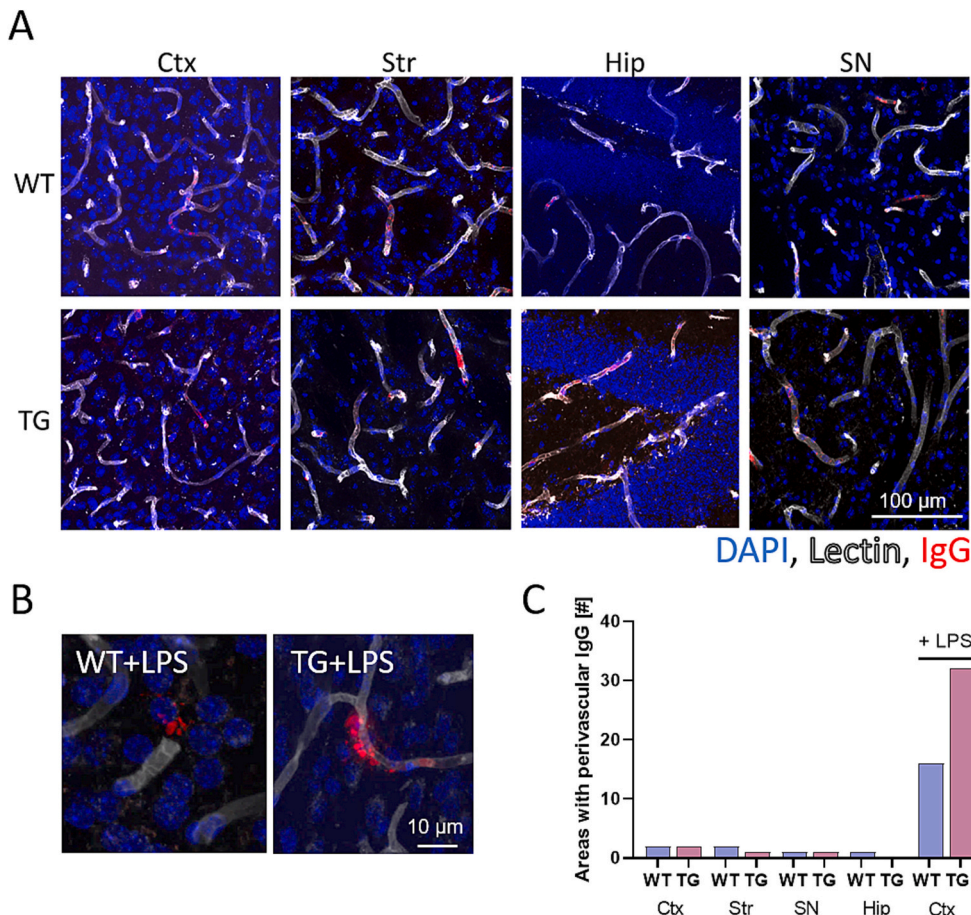


Fig. 5. Capillary immunoglobulin G (IgG) extrusion analysis in brains of 6 months old Thy1-aSyn animals. (A) Representative confocal images of IgG (red) and capillary lectin (white) staining in different brain regions (Ctx: cortex, Str: striatum, SN: substantia nigra, Hip: hippocampus) of Thy1-aSyn (TG) and wild-type (WT) animals (n = 8 animals) to study IgG extravasation as a measure of blood-brain barrier leakiness. Cortices of mice (Thy1-aSyn and WT) injected with LPS (0.8 mg/kg, 3 days after i.p. injection) served as positive control. Magnified areas with perivascular IgG leakage in LPS controls are shown in B. (C) Diagram showing areas of perivascular IgG leakage detected by microscopical analysis of different brain regions using two brain slices per animal and region. Perivascular IgG deposition was detected in LPS injected control animals but not/only rarely in WT or Thy1-aSyn mice. LPS: lipopolysaccharide. (For interpretation of the references to colour in this figure legend, the reader is referred to the web version of this article.)

(Fig. 4C). Moreover, exemplary immunofluorescent staining of isolated striatal capillaries of a wild-type and Thy1-aSyn mouse (2 months of age) for ZO-1 showed continuous tight junction strands along the capillaries indicating structural integrity and absence of structural changes of ZO-1 (Fig. 4C).

3.6. No overt BBB immunoglobulin G leakage in Thy1-aSyn mice

Compromised integrity of the BBB can promote neuronal injury and neuroinflammation (Alvarez et al., 2015; Brochard et al., 2009; Gray and Woulfe, 2015). In order to measure BBB permeability in Thy1-aSyn mice immunostaining for blood-derived IgG and endothelial lectin was used to examine IgG extravascular deposition as measure for BBB leakiness. Microscopic analysis of several brain regions including cortex, striatum, hippocampus and substantia nigra of 6 months old Thy1-aSyn mice compared to age-matched wild-type controls ($n = 8/\text{group}$) showed no increased IgG (~150 kDa) permeation across the BBB in Thy1-aSyn mice (Fig. 5A). In contrast, a single i.p. injection of low dose bacterial toxin lipopolysaccharide (LPS) showed extravascular IgG deposition in wild-type and Thy1-aSyn mice (Fig. 5B,C), indicative for BBB leakiness.

4. Discussion

Our data supports alterations of key BBB-related proteins in isolated capillaries from striatum and cortex of Thy1-aSyn mice at two prodromal stages of disease progression. BBB alterations observed in striatal capillaries from Thy1-aSyn mice include reduced vessel density, reduced aquaporin-4 coverage, reduced P-gp expression, increased LRP1 expression, increased pS129-alpha-synuclein deposition, increased VCAM-1 and MMP-3 expression and early reduction in tight junction protein occludin (summarized in Fig. 6). Interestingly, cortical capillaries do not decrease significantly in density, but show reduced aquaporin-4 expression. While there is no overt genotype effect on P-gp and LRP1 expression in cortical capillaries, pS129-alpha-synuclein accumulation is present. Furthermore cortical capillaries upregulate ICAM-1 instead of VCAM-1 in Thy1-aSyn mice. With age, MMP-3 and

ZO-1 are downregulated in cortical regions but occludin and claudin-5 are upregulated. These alterations of BBB integrity lead, however, not to an overt IgG leakage in brain parenchyma, which only occurs at additional impact of a toxin as demonstrated with a single application of LPS for the cortex.

These results are in line with observations that in absence of overt and wide-spread leakiness of the BBB in PD patients, there are observable alterations which could favor transition of molecules, as shown for verapamil in de novo PD (Bartels et al., 2008; Kortekaas et al., 2005). Post-mortem pathology of PD brains revealed alterations of the microstructure of vessels such as a thickening of the basal lamina (Farkas et al., 2000) and vessel degeneration, which was found in multiple brain regions but particularly in the substantia nigra, middle frontal cortex and brain stem nuclei (Guan et al., 2013). Careful histological analysis revealed compromised BBB integrity in the striatum of PD patients including erythrocyte extravasation, perivascular hemosiderin, and leakage of various serum proteins, pointing to some leakiness in advanced PD (Gray and Woulfe, 2015). If BBB alterations occur early in PD and extend to cortical brain regions, then it is unlikely that they develop merely in response to nigrostriatal neurodegeneration. Among others, widespread alpha-synuclein pathology could represent a contributing factor, which is present in Thy1-aSyn mice at the ages tested.

BBB alterations in Thy1-aSyn mice were detected already at 2 months of age and remain stable up to 6 months. This indicates that pathogenesis of these alterations is linked to early pathology, such as pS129-alpha-synuclein accumulation, initial formation of proteinase K resistant aggregates in striatum and cortex, and microgliosis in the striatum (Richter et al., 2023). Of note, while alpha-synuclein overexpression is widespread, microgliosis occurs first in the striatum compared to substantia nigra and cortex (Watson et al., 2012). At 6 months of age Thy1-aSyn mice represent a model of prodromal PD with motor and non-motor dysfunction, alpha-synuclein pathology, overt nigrostriatal microgliosis, increased extracellular dopamine and dopamine metabolism and decreased dopaminergic synaptic density in the striatum, among other phenotypes, while dopamine loss becomes significant at 14–16 months of age (Richter et al., 2023).

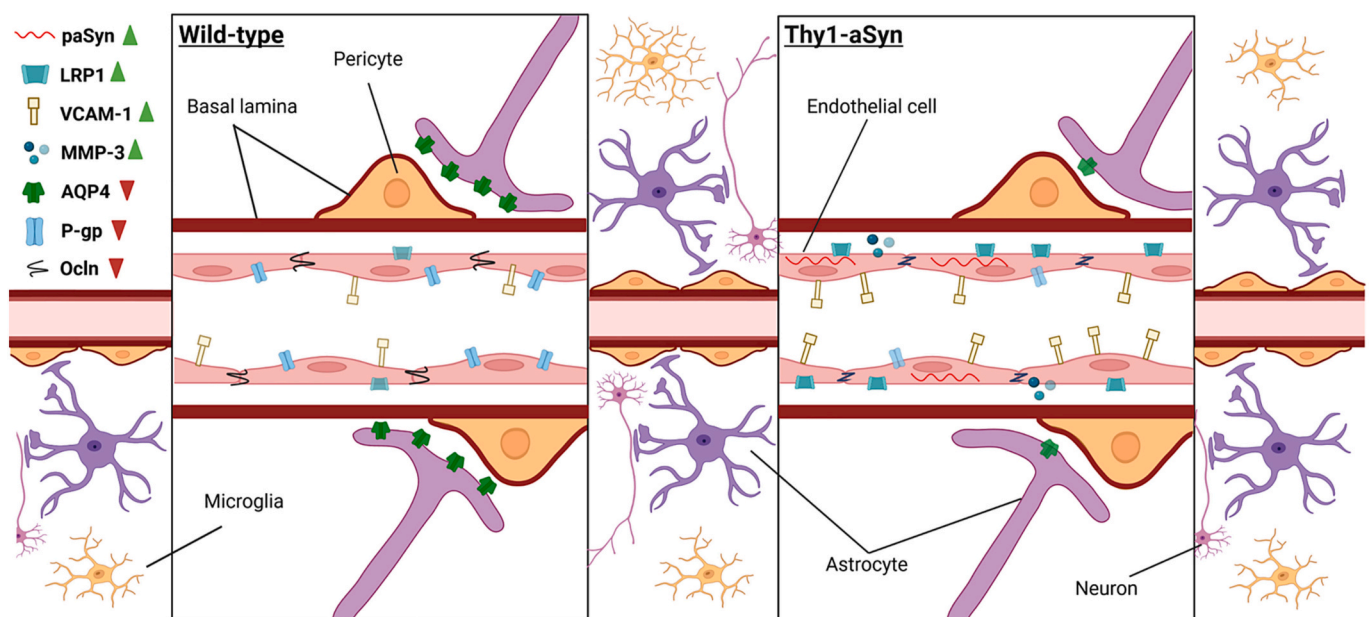


Fig. 6. Schematic representation of blood-brain barrier alterations in striatal capillaries of Thy1-aSyn mice (right box) compared to wild-type animals (left box). Arrows indicate the alterations occurring in the Thy1-aSyn mice. Observed alterations include accumulation of pS129-alpha-synuclein, increased expression of LRP1, VCAM-1 and MMP-3, reduced AQP4 coverage and reduction in P-gp and tight junction protein occludin. paSyn: pS129-alpha-synuclein, LRP1: low-density lipoprotein receptor-related protein 1, VCAM-1: vascular cell adhesion molecule 1, MMP-3: matrix metalloprotease-3, AQP4: aquaporin-4, P-gp: P-glycoprotein, Occludin: occludin. (Created with BioRender).

We specifically demonstrate pS129-alpha-synuclein in isolated brain capillaries in Thy1-aSyn mice at 2 and 6 months of age. In Thy1-aSyn mice, human alpha-synuclein is overexpressed and pS129-alpha-synuclein accumulates in neurons across the brain (Chesselet et al., 2012; Richter et al., 2023). Thus, it is most probable that alpha-synuclein and its post-translational modification in endothelial cells are derived from brain parenchyma, e.g. via LRP1 mediated efflux (Sui et al., 2014). Alpha-synuclein may be transported across the BBB as part of a physiological process, but also as mechanism for clearance as shown for beta amyloid and tau (Clarke-Bland et al., 2022; Sui et al., 2014). The observed higher expression of LRP1 in Thy1-aSyn brain capillaries has previously been described in brain tissue of PD and incidental Lewy body disease patients (Wilhelmus et al., 2011). This could represent a clearance response to alpha-synuclein accumulation in brain tissue, as alpha-synuclein is a substrate for LRP1 mediated efflux (Sui et al., 2014). While there was no evidence for P-gp to be involved in alpha-synuclein transport across the blood-brain barrier (Sui et al., 2014), P-gp function seems to be decreased in human brains of PD patients (Bartels et al., 2008; Kortekaas et al., 2005). Presumably toxic pS129-alpha-synuclein and formation of aggregated protein could trigger inflammatory and stress responses in endothelial cells that can impact BBB integrity (Fujiwara et al., 2002). This is supported by the increased expression of cell adhesion molecules ICAM-1 or VCAM-1 in capillaries of Thy1-aSyn mice, which mediate leukocyte-endothelial adherence (Engelhardt and Ransohoff, 2012). Furthermore, pericytes can become reactive and secrete cytokines and matrix metalloproteases that can have detrimental effects on BBB integrity (Dohgu et al., 2019; Herland et al., 2016). These molecular mechanisms are evident in alterations in matrix metalloproteases and tight junction proteins observed in isolated capillaries, encompassing endothelial cells and pericytes (Fig. 1D,E), in Thy1-aSyn mice.

Microgliosis and release of cytokines including TNF- α , IL-1 β and IL-6 are well described in brains of PD patients and Thy1-aSyn mice (Liu et al., 2022; Mogi et al., 1994; Watson et al., 2012). Importantly, microgliosis develops first in the striatum in Thy1-aSyn mice (Watson et al., 2012), which could explain why the striatal BBB appears more affected compared to the cortex. Microgliosis could be an additional aggravating factor towards BBB dysfunction, as observed in PD models injected with neurotoxins that develop microgliosis together with BBB leakiness and decreased levels of the tight junction proteins occludin and ZO-1 (Chen et al., 2008) or increased expression of P-gp and beta 3-integrin (Carvey et al., 2005). Microglia and astroglia display intricate communication at the neurovascular unit. Accumulation of alpha-synuclein in astroglia is thought to contribute to astroglia dysfunction including BBB dysregulation (Kam et al., 2020). Aquaporin-4 mediates the communication between microglia and astroglia (Sun et al., 2016), and the here observed reduction in aquaporin-4 in several brain regions indicates an alteration of the microglia-astroglia-vascular coupling (Halder and Milner, 2020). Specifically, downregulation of aquaporin-4 represents a loss of structural integrity at the astroglia endfeet, which in turn results in loss of their ability to support the BBB integrity (Haruwaka et al., 2019; Zeppenfeld et al., 2017; Zhou et al., 2008). Disruption of astrocytes in PD and in Alzheimer's disease correlates with BBB leakiness (Abbott et al., 2006). Moreover, aquaporin-4 dispersion from endfeet has previously been linked to Alzheimer's disease pathogenesis and may reduce the clearance of beta amyloid and tau (Clarke-Bland et al., 2022).

Histological analysis of brain sections from mice over-expressing A53T mutated (under the prion promotor) or wild-type alpha-synuclein (under the (BAC)-alpha-synuclein-green fluorescent protein (GFP) construct) also reported decreased expression of tight junction proteins. Conversely to our observations in Thy1-aSyn mice at prodromal stage, alterations of microstructure led to an overt leakage of the BBB in these models (Elabi et al., 2021; Lan et al., 2022). As we observed decrease in lectin-positive vessel density in the striatum, there may be subtle leakage, which we did not detect with the IgG staining here, or by

quantifying invading immune cells previously (Watson et al., 2012). This is a major limitation of the study, as smaller molecules such as sucrose or sodium fluorescein would detect subtle leakage more reliable. However, as discussed above, current imaging and post-mortem studies in PD patients do not suggest an overt BBB leakiness for blood cells, especially in prodromal PD. Importantly, as demonstrated by induction of IgG leakiness upon a single low dose LPS injection in our study, a compromised BBB could be more prone to open to peripheral immune cells upon toxin exposure. Of note, changes in expression levels of receptors for LPS could increase the sensitivity of Thy1-aSyn mice to this bacterial toxin. Thy1-aSyn mice show increased Toll-like receptor 4 levels in the substantia nigra at 5–6 months, an important receptor mediating LPS toxicity (Qureshi et al., 1999; Watson et al., 2012). Future studies will determine the exact cell types with higher Toll-like receptor expression, including assessment of all components of the neurovascular unit. This would expose the brain parenchyma to detrimental toxins, cytokines and invading macrophages. In addition, the decrease of P-gp protein in striatal brain capillaries of Thy1-aSyn mice can lead to an elevated toxin exposure of brain cells (Kortekaas et al., 2005). Invasion of toxins or immune cells would enhance the above discussed inflammatory reactivity at the neurovascular unit, mediated by endothelial cells, pericytes or glia, and further damage the BBB, and thereby enhance neuropathology.

Thus, preventing or counteracting BBB alteration represents an underutilized target for disease modification, especially early in disease progression. Interestingly, deep brain stimulation appears to upregulate microvessel endothelial cell thickness, length and density as well as tight junction-associated proteins. This was accompanied by decreased microgliosis and increase in vascular endothelial growth factor (VEGF), which was interpreted as BBB stabilizing response (Pienaar et al., 2015). Conversely, in A53T alpha-synuclein overexpressing mice, release of VEGFA by astroglia increased and application of a VEGFA receptor antagonist ameliorated BBB pathology in this model (Lan et al., 2022). These studies demonstrate that BBB alterations can be normalized by targeted treatment.

5. Conclusions

Alpha-synuclein overexpression leads to progressive and regionally specific alterations of the BBB in prodromal Thy1-aSyn mice, which may progress to leakiness upon additional impacts or with advanced disease. This provides a useful tool for further research into the molecular mechanisms of BBB alterations in PD to propose rational treatment targets. Our data opens the possibility that targeting alpha-synuclein pathology in cells beyond neurons may benefit the BBB integrity. Furthermore, pre-clinical and clinical studies need to take into consideration that systemically applied compounds or antibodies will need to cross the BBB and thereby potentially encounter alpha-synuclein decomposition in endothelial and glia cells.

Funding

The study was funded by intramural funds with no role in design, analysis, interpretation or writing of the manuscript. This Open Access publication was funded by the Deutsche Forschungsgemeinschaft (DFG, German Research Foundation) - 491094227 "Open Access Publication Funding" and the University of Veterinary Medicine Hannover, Foundation.

Authors' contributions

The study was conceived and designed by B.G. and F.R., experiments and data analyses were carried out by K.L., L.T.P. and B.G., the article was primarily written by F.R. and B.G. with contributions from K.L. and L.T.P.. All authors read and approved the final manuscript.

CRedit authorship contribution statement

Kristina Lau: Investigation, Formal analysis, Visualization, Writing – review & editing. **Lisa T. Porschen:** Investigation, Formal analysis, Visualization, Writing – review & editing. **Franziska Richter:** Conceptualization, Funding acquisition, Supervision, Writing – original draft, Writing – review & editing. **Birthe Gericke:** Conceptualization, Investigation, Formal analysis, Visualization, Writing – original draft, Writing – review & editing.

Declaration of Competing Interest

The authors declare that they have no competing interests.

Data availability

The datasets used and/or analyzed during the current study available from the corresponding author on reasonable request.

Acknowledgements

The authors are grateful to Andrea Ofner, Edith Kaczmarek and Ivo Wiesweg for excellent technical assistance.

Appendix A. Supplementary data

Supplementary data to this article can be found online at <https://doi.org/10.1016/j.nbd.2023.106298>.

References

- Abbott, N.J., 2013. Blood-brain barrier structure and function and the challenges for CNS drug delivery. *J. Inher. Metab. Dis.* 36, 437–449.
- Abbott, N.J., et al., 2006. Astrocyte-endothelial interactions at the blood-brain barrier. *Nat. Rev. Neurosci.* 7, 41–53.
- Alvarez, J.I., et al., 2015. Focal disturbances in the blood-brain barrier are associated with formation of neuroinflammatory lesions. *Neurobiol. Dis.* 74, 14–24.
- van Assema, D.M., et al., 2012. P-glycoprotein function at the blood-brain barrier: effects of age and gender. *Mol. Imaging Biol.* 14, 771–776.
- Bartels, A.L., et al., 2008. Decreased blood-brain barrier P-glycoprotein function in the progression of Parkinson's disease, PSP and MSA. *J. Neural Transm. (Vienna)* 115, 1001–1009.
- Brochard, V., et al., 2009. Infiltration of CD4+ lymphocytes into the brain contributes to neurodegeneration in a mouse model of Parkinson disease. *J. Clin. Invest.* 119, 182–192.
- Buzhdygan, T.P., et al., 2020. The SARS-CoV-2 spike protein alters barrier function in 2D static and 3D microfluidic in-vitro models of the human blood-brain barrier. *Neurobiol. Dis.* 146, 105131.
- Carvey, P.M., et al., 2005. 6-Hydroxydopamine-induced alterations in blood-brain barrier permeability. *Eur. J. Neurosci.* 22, 1158–1168.
- Chen, X., et al., 2008. Caffeine protects against MPTP-induced blood-brain barrier dysfunction in mouse striatum. *J. Neurochem.* 107, 1147–1157.
- Chesselet, M.F., et al., 2012. A progressive mouse model of Parkinson's disease: the Thy1-aSyn ("line 61") mice. *Neurotherapeutics.* 9, 297–314.
- Chiu, S.Y., et al., 2022. Lewy body dementias: controversies and drug development. *Neurotherapeutics.* 19, 55–67.
- Chung, Y.C., et al., 2013. MMP-3 contributes to nigrostriatal dopaminergic neuronal loss, BBB damage, and neuroinflammation in an MPTP mouse model of Parkinson's disease. *Mediat. Inflamm.* 2013, 370526.
- Clarke-Bland, C.E., et al., 2022. Emerging roles for AQP in mammalian extracellular vesicles. *Biochim. Biophys. Acta Biomembr.* 1864, 183826.
- Daneman, R., et al., 2010. Pericytes are required for blood-brain barrier integrity during embryogenesis. *Nature.* 468, 562–566.
- Devos, D., et al., 2021. Seven solutions for neuroprotection in Parkinson's disease. *Mov. Disord.* 36, 306–316.
- Dohgu, S., et al., 2019. Monomeric alpha-synuclein induces blood-brain barrier dysfunction through activated brain pericytes releasing inflammatory mediators in vitro. *Microvasc. Res.* 124, 61–66.
- Dorsey, E.R., Bloem, B.R., 2018. The Parkinson pandemic—a call to action. *JAMA Neurol.* 75, 9–10.
- Edwards, T.L., et al., 2010. Genome-wide association study confirms SNPs in SNCA and the MAPT region as common risk factors for Parkinson disease. *Ann. Hum. Genet.* 74, 97–109.
- Elabi, O., et al., 2021. Human alpha-synuclein overexpression in a mouse model of Parkinson's disease leads to vascular pathology, blood brain barrier leakage and pericyte activation. *Sci. Rep.* 11, 1120.
- Engelhardt, B., Ransohoff, R.M., 2012. Capture, crawl, cross: the T cell code to breach the blood-brain barriers. *Trends Immunol.* 33, 579–589.
- Farkas, E., et al., 2000. Pathological features of cerebral cortical capillaries are doubled in Alzheimer's disease and Parkinson's disease. *Acta Neuropathol.* 100, 395–402.
- Fujiwara, H., et al., 2002. Alpha-Synuclein is phosphorylated in synucleinopathy lesions. *Nat. Cell Biol.* 4, 160–164.
- Gatto, N.M., et al., 2010. Alpha-Synuclein gene may interact with environmental factors in increasing risk of Parkinson's disease. *Neuroepidemiology.* 35, 191–195.
- Gericke, B., et al., 2020. A face-to-face comparison of claudin-5 transduced human brain endothelial (hCMEC/D3) cells with porcine brain endothelial cells as blood-brain barrier models for drug transport studies. *Fluids Barriers CNS* 17, 53.
- Gerstenberger, J., et al., 2016. The novel adaptive rotating beam test unmasks sensorimotor impairments in a transgenic mouse model of Parkinson's disease. *Behav. Brain Res.* 304, 102–110.
- Gray, M.T., Wouffe, J.M., 2015. Striatal blood-brain barrier permeability in Parkinson's disease. *J. Cereb. Blood Flow Metab.* 35, 747–750.
- Guan, J., et al., 2013. Vascular degeneration in Parkinson's disease. *Brain Pathol.* 23, 154–164.
- Halder, S.K., Milner, R., 2020. Mild hypoxia triggers transient blood-brain barrier disruption: a fundamental protective role for microglia. *Acta Neuropathol. Commun.* 8, 175.
- Hartlage-Rubsamen, M., et al., 2021. A glutaminyl cyclase-catalyzed alpha-synuclein modification identified in human synucleinopathies. *Acta Neuropathol.* 142, 399–421.
- Hartz, A.M., et al., 2012. Amyloid-beta contributes to blood-brain barrier leakage in transgenic human amyloid precursor protein mice and in humans with cerebral amyloid angiopathy. *Stroke.* 43, 514–523.
- Haruwaka, K., et al., 2019. Dual microglia effects on blood brain barrier permeability induced by systemic inflammation. *Nat. Commun.* 10, 5816.
- Herland, A., et al., 2016. Distinct contributions of astrocytes and Pericytes to Neuroinflammation identified in a 3D human blood-brain barrier on a Chip. *PLoS One* 11, e0150360.
- Hou, Y., et al., 2019. Ageing as a risk factor for neurodegenerative disease. *Nat. Rev. Neurol.* 15, 565–581.
- Huang, Y., et al., 2011. Interaction between α -Synuclein and tau genotypes and the progression of Parkinson's disease. *J. Parkinsons Dis.* 1, 271–276.
- Kam, T.I., et al., 2020. Microglia and astrocyte dysfunction in parkinson's disease. *Neurobiol. Dis.* 144, 105028.
- Kortekaas, R., et al., 2005. Blood-brain barrier dysfunction in parkinsonian midbrain in vivo. *Ann. Neurol.* 57, 176–179.
- Lan, G., et al., 2022. Astrocytic VEGFA: an essential mediator in blood-brain-barrier disruption in Parkinson's disease. *Glia.* 70, 337–353.
- Liu, S.Y., et al., 2022. Brain microglia activation and peripheral adaptive immunity in Parkinson's disease: a multimodal PET study. *J. Neuroinflammation* 19, 209.
- Luissint, A.C., et al., 2012. Tight junctions at the blood brain barrier: physiological architecture and disease-associated dysregulation. *Fluids Barriers CNS* 9, 23.
- McCann, H., et al., 2014. Alpha-Synucleinopathy phenotypes. *Parkinsonism Relat. Disord.* 20 (Suppl. 1), S62–7.
- McClain, J.A., et al., 2009. Increased MMP-3 and CTGF expression during lipopolysaccharide-induced dopaminergic neurodegeneration. *Neurosci. Lett.* 460, 27–31.
- Miller, D.S., et al., 2000. Xenobiotic transport across isolated brain microvessels studied by confocal microscopy. *Mol. Pharmacol.* 58, 1357–1367.
- Mogi, M., et al., 1994. Tumor necrosis factor- α (TNF- α) increases both in the brain and in the cerebrospinal fluid from parkinsonian patients. *Neurosci. Lett.* 165, 208–210.
- Partridge, W.M., 1999. Blood-brain barrier biology and methodology. *J. Neuro-Oncol.* 5, 556–569.
- Pienaar, I.S., et al., 2015. Deep-brain stimulation associates with improved microvascular integrity in the subthalamic nucleus in Parkinson's disease. *Neurobiol. Dis.* 74, 392–405.
- Puris, E., et al., 2022. Altered protein expression of membrane transporters in isolated cerebral microvessels and brain cortex of a rat Alzheimer's disease model. *Neurobiol. Dis.* 169, 105741.
- Qureshi, S.T., et al., 1999. Endotoxin-tolerant mice have mutations in toll-like receptor 4 (Tr4). *J. Exp. Med.* 189, 615–625.
- Rempe, R.G., et al., 2018. Matrix metalloproteinase-mediated blood-brain barrier dysfunction in epilepsy. *J. Neurosci.* 38, 4301–4315.
- Richter, F., et al., 2023. A mouse model to test novel therapeutics for Parkinson's disease: an update on the Thy1-aSyn ("line 61") mice. *Neurotherapeutics.* 20, 97–116.
- Schindelin, J., et al., 2012. Fiji: an open-source platform for biological-image analysis. *Nat. Methods* 9, 676–682.
- Schidlitzki, A., et al., 2023. Double-edged effects of venglustat on behavior and pathology in mice overexpressing alpha-synuclein. *Mov Disord.* 38 (6), 1044–1055.
- Spillantini, M.G., et al., 1997. Alpha-synuclein in Lewy bodies. *Nature.* 388, 839–840.
- Spillantini, M.G., et al., 1998. Alpha-Synuclein in filamentous inclusions of Lewy bodies from Parkinson's disease and dementia with Lewy bodies. *Proc. Natl. Acad. Sci. U. S. A.* 95, 6469–6473.
- Storck, S.E., et al., 2021. Brain endothelial LRP1 maintains blood-brain barrier integrity. *Fluids Barriers CNS* 18, 27.
- Sui, Y.T., et al., 2014. Alpha synuclein is transported into and out of the brain by the blood-brain barrier. *Peptides.* 62, 197–202.
- Sun, H., et al., 2016. Aquaporin-4 mediates communication between astrocyte and microglia: implications of neuroinflammation in experimental Parkinson's disease. *Neuroscience.* 317, 65–75.

- Watson, M.B., et al., 2012. Regionally-specific microglial activation in young mice over-expressing human wildtype alpha-synuclein. *Exp. Neurol.* 237, 318–334.
- Wilhelmus, M.M., et al., 2011. Apolipoprotein E and LRP1 increase early in Parkinson's disease pathogenesis. *Am. J. Pathol.* 179, 2152–2156.
- Willott, E., et al., 1992. Localization and differential expression of two isoforms of the tight junction protein ZO-1. *Am. J. Phys.* 262, C1119–C1124.
- Zeppenfeld, D.M., et al., 2017. Association of Perivascular Localization of Aquaporin-4 with cognition and Alzheimer disease in aging brains. *JAMA Neurol.* 74, 91–99.
- Zeuner, K.E., et al., 2019. Progress of pharmacological approaches in Parkinson's disease. *Clin. Pharmacol. Ther.* 105, 1106–1120.
- Zhao, Z., et al., 2015. Establishment and dysfunction of the blood-brain barrier. *Cell.* 163, 1064–1078.
- Zhou, J., et al., 2008. Altered blood-brain barrier integrity in adult aquaporin-4 knockout mice. *Neuroreport.* 19, 1–5.